Excitation Function for the $C^{12}(\pi^-,\pi^-n)C^{11}$ Reaction*

PAUL L. REEDER† AND SAMUEL S. MARKOWITZ
Lawrence Radiation Laboratory, University of California, Berkeley, California
(Received 21 August 1963)

The excitation function for the reaction $C^{12}(\pi^-,\pi^-n)C^{11}$ was measured from 53 to 1610 MeV by bombarding targets of plastic scintillator with pions. The intensity of the pion beam was monitored with a two-counter telescope and 40-Mc/sec scaling system. The scintillator target was mounted on a phototube and became the detector for the C^{11} positron activity. Corrections were made for muon contamination in the beam, coincidence losses in the monitor system, C^{11} activity produced by stray background at the accelerator, C^{11} activity produced by secondaries in the target, and the efficiency of the C^{11} detection system. The $C^{12}(\pi^-,\pi^-n)C^{11}$ cross sections rise from a threshold at about 50 MeV to a peak of about 70 mb at 190 MeV after which they decrease to 30 mb at 373 MeV and are relatively constant at higher energies. The (π^-,π^-n) peak occurs at the same energy as the resonance in free-particle π^-n scattering at 190 MeV. Calculations based on a "knock-on collision" mechanism and "sharp-cutoff" nuclear density reproduce the shape of the experimental excitation function, but the magnitudes of the calculated cross sections are low by a factor of about 5 or 6. This simple model indicates that the $C^{12}(\pi^-,\pi^-n)C^{11}$ reaction occurs in the nuclear surface region at all bombarding energies.

I. INTRODUCTION

A NUMBER of experiments have shown the existence of quasifree scattering of pions from individual nucleons within nuclei.[1–3] In general, these experiments measured the characteristics of the outgoing pion rather than those of the residual nucleus. Because the $J=T=\frac{3}{2}$ resonance in π^-n scattering is so pronounced, we expect that the excitation functions for simple nuclear reactions of the type $Z^A(\pi^-,\pi^-n)Z^{A-1}$ must also show a resonance peak, provided the reaction mechanism consists of a single collision between the incident pion and a neutron within the target nucleus. The recoil partners from this collision must escape from the nucleus without depositing sufficient excitation energy to evaporate additional nucleons.

This mechanism implies that the effective cross section for π^-n collisions within nuclei is the dominating factor in determining the cross section for a given (π^-,π^-n) reaction. The effective cross section differs from the free-particle cross section because some collisions are forbidden by the Pauli exclusion principle; in addition, the momentum distribution of nucleons within the nucleus tends to broaden the sharp resonances in the free-particle cross sections.

The reaction $C^{12}(\pi^-,\pi^-n)C^{11}$ was chosen to test these ideas because a simple and efficient technique for measuring the C^{11} activity was available. The cross section for the formation of C^{11} from C^{12} was measured as a function of incident pion energy at 1610 MeV and near the $J=T=\frac{3}{2}$ free-particle resonance region at 200 MeV.

II. EXPERIMENTAL PROCEDURE

Except for one experiment with 1610-MeV pions at the Bevatron, the $C^{12}(\pi^-,\pi^-n)C^{11}$ excitation function was measured with the meson beams at the Berkeley 184-in. cyclotron. Targets of plastic scintillator were bombarded with a monitored beam of pions, and the amount of C^{11} produced was determined by internal scintillation counting of the C^{11} positron activity.[4,5] The targets consisted of 2.5-in.-diam by 1-in.-thick disks of plastic scintillator (a mixture of polystyrene, 97%; terphenyl, 3%; and tetraphenyl butadiene, 0.07%).

A. Pion Beams at the 184-in. Cyclotron

The pion beams set up for many different experiments were used for this work. (The physicists responsible for these beams are listed in the Acknowledgment section.) A representative physics experiment involved the bombardment of a liquid-hydrogen target with pions. The beam setup for the 380-MeV π^- beam, typical of many of the experiments, is shown in Fig. 1. The pion beam passed through the hydrogen target and irradiated the plastic scintillator target at a given distance downstream. The quadrupole magnet before the bending magnet focused the pions at the liquid-hydrogen target. The pion energies at the magnet focus were determined by the physicists responsible for the beam by wire-orbit analysis of the bending magnet and by range curves in Cu and CH_2. The range curves also provided information on the composition of the beam at the hydrogen target. The energy-loss tables of Rich and Madey were used to calculate the energy lost by the pions in traveling from the midpoint of the hydrogen target to the midpoint of the plastic-scintillator target.[6] The momen-

* Work done under the auspices of the U. S. Atomic Energy Commission.
† Present address, Chemistry Department, Brookhaven National Laboratory, Upton, L. I., New York.
[1] A. E. Ignatenko, in CERN Symp. High Energy Accelerators Pion Phys., Geneva, 1956, Proc. 2, 313 (1956).
[2] T. A. Fujii, Phys. Rev. 113, 695 (1959).
[3] T. Fowler and K. Watson, Nucl. Phys. 13, 549 (1959).
[4] J. Cumming, G. Friedlander, and C. Swartz, Phys. Rev. 111, 1386 (1958).
[5] J. Cumming and R. Hoffman, Rev. Sci. Instr. 29, 1104 (1958).
[6] M. Rich and R. Madey, Range-Energy Tables, University of California, Lawrence Radiation Laboratory Report UCRL-2301, 1954 (unpublished).

TABLE I. Dimensions of monitor counters.

Counter	Type	Surface dimensions (in.)	Thickness (in.)
A	Square	3.50×3.50	0.25
B	Circular disk	2.50 diam	0.25
C	Circular disk	2.50 diam	1.00

tum spread of pion beams greater than 200 MeV was usually about 1 to 3%. At 127 MeV, the momentum spread was about 7%, and at lower energies the momentum spread was as high as 10%. The energy lost by a pion passing through the 1-in.-thick plastic scintillator was combined by root-mean-square addition with the energy spread of the beam to determine the over-all energy spread.

B. Beam Monitor System

The pion beam was monitored with two plastic-scintillator detectors A and B attached by Lucite light pipes to RCA 6810A photomultiplier tubes (see Fig. 2). The third counter C was used as a beam monitor while plateau curves and delay curves for the coincidence system were measured. The dimensions of each counter are given in Table I. The targets, attached to the backside of counter B, had the same diameter as counter B, so that this counter defined the beam size. Because the beam was slightly divergent in moving from counter A to counter B and because counter A was larger than counter B, all the pions passing through counter B and the target also passed through counter A. The three counters were mounted about 6 to 8 in. apart on an aluminum frame, and their positions could be adjusted to meet varying conditions of space and beam height.

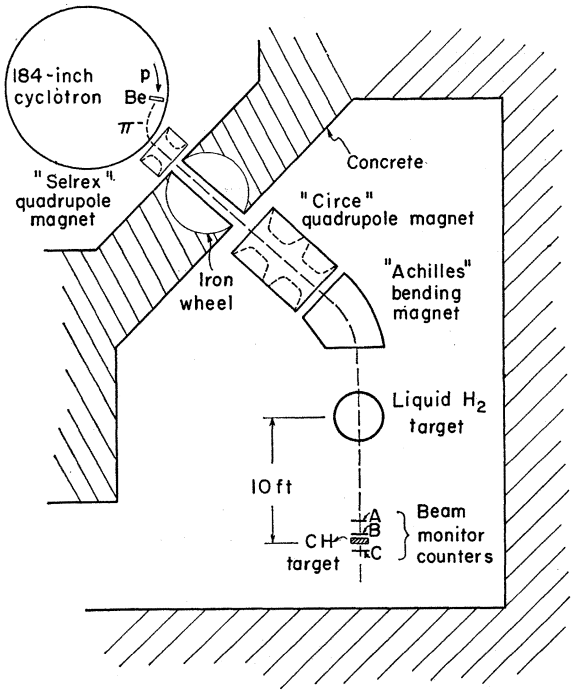

FIG. 1. Experimental setup at 184-in. cyclotron for 380-MeV π^- beam.

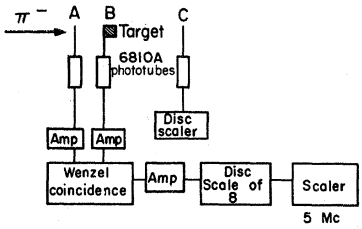

FIG. 2. Electronics for 40-Mc/sec beam-monitor system.

The tube bases for counters A and B were designed for use with high-intensity beams, as described by Mollenauer.[7] After suitable amplification, the pulses from counters A and B were led to a Wenzel coincidence unit with a resolving time of 8 nsec. The output of the coincidence unit went to a 40-Mc/sec discriminator and scale-of-eight unit.

Even with a high-speed counting system, the monitor system had to be corrected for coincidence losses (accidentals) that occur when two or more pions pass through the counter telescope simultaneously. The cyclotron beam came in 13-nsec bursts, 54 nsec apart, so the accidentals correction was determined empirically by inserting a 54-nsec delay into one of the input channels of the coincidence unit. The accidentals counting rate was measured before and after a target bombardment and was added to the average counting rate determined with normal delays during the bombardment. The sum of the accidental and normal counting rates was linearly related to the intensity of the internal proton beam. Because the pion-beam intensity varied from setup to setup, the accidentals correction varied from 0 to 10% of the pion-beam intensity at different energies.

The beam-monitor intensity was also corrected for the contamination of the π^- beam with μ^- and e^-. Muons produced by pion decay before the bending magnet and having the same momentum as the pions were distinguished by range curves. The fraction of the beam due to muons produced downstream from the bending magnet was calculated directly. The electron contamination determined by the range curves was usually less than 2% of the total beam. The total μ^- and e^- contamination varied from about 40% of the total beam at 50 MeV to about 8% at 373 MeV. Plastic scintillators, when bombarded with low-energy beams (<50 MeV) of μ^- and e^-, gave negligible amounts of C^{11} activity. The low μ^- and e^- beam intensity meant that only an upper limit could be placed on the cross section for C^{11} production by μ^- and e^-. We estimate this cross section to be less than 1.6 mb. The pion-beam intensity was corrected for the fraction of the beam that was μ^- and e^-, but the production of C^{11} by μ^- and e^- was neglected.

[7] J. Mollenauer, Phys. Rev. **127**, 867 (1962).

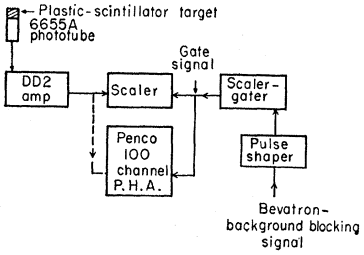

FIG. 3. Electronics for C^{11} detection system.

C. Bevatron Experiment

One experiment was performed at the Bevatron with 1610-MeV pions. The counter telescope previously described was not used. The physics experimenters used their own counter telescope to determine the average number of pions per pulse. The average beam intensity for the plastic-scintillator bombardment was estimated from this number and the total number of pulses through the target. Although the pion intensity was considerably less than the intensities at the 184-in. cyclotron, an initial C^{11} activity of 135 counts per min above a natural background of 135 counts per min was obtained.

D. Detection System for C^{11}

After irradiation at the accelerator, the plastic-scintillator targets were brought back to the Chemistry Building, where the detection equipment was arranged to follow the C^{11} decay. Targets were not counted at the cyclotron because of the large and erratic background at the machine. The plastic scintillator was attached to an RCA 6655A photomultiplier tube with Dow-Corning 200 silicone grease and covered with a light-tight container. The principal units of the counting system are shown in Fig. 3. All pulses above a fixed discriminator level were sent directly to a scaler and a decay curve was obtained. The 100-channel pulse-height analyzer was used to display the spectrum of pulses from the DD2 linear amplifier. Comparison of the spectra obtained after pion bombardments with spectra from standard β^- sources showed that the observed target spectra conformed to that expected from C^{11}.

The scaler-gater system was required to reduce the background caused by the Bevatron. The scaler-gater turned the scaler off for the short period of time in which bursts from the Bevatron were observed. The background could be reduced from 230 counts per min to 135 counts per min, with an off-time of 3.3%.

The scaling system was standardized by counting an external (2π geometry) Cs^{137} β^- source before each run. The discriminator of the scaler was held constant, and the gain of the amplifier was adjusted to give a fixed counting rate with this source.

After subtraction of the natural background, the decay curve obtained with this scaling system showed no component other than the 20.4-min activity due to C^{11}. The initial activity of C^{11} was obtained by extrapolating the decay curve back to end-of-bombardment time. Most of the data were obtained with initial activities of a few thousand counts per min, but initial activities as high as 47 000 counts per min and as low as 135 counts per min were also measured.

The efficiency of the C^{11} detection system was determined by a β-γ coincidence method described by Cumming and Hoffman.[5] The high-activity C^{11} source needed for coincidence counting was made by bombarding one of the plastic-scintillator targets with the external proton beam at the 184-in. cyclotron. The "fast-slow" coincidence system had a resolving time of about 80 nsec and recorded the β singles counting rate, γ singles counting rate, and β–γ coincidence counting rate. After appropriate corrections, the product of the singles counting rates divided by the β–γ coincidence rate gave the disintegration rate. The observed counting rate in the C^{11} detection system divided by the disintegration rate gave the efficiency of the C^{11} detection system. Seven measurements of the efficiency gave an average value of $(83\pm3)\%$.

E. Corrections to Initial Activity

The meson cave at the 184-in. cyclotron has a background of fast neutrons and other particles that might contribute to the production of C^{11}. The effect of this background radiation was measured by placing an identical plastic scintillator at a distance of 1 ft from the beam. The activity in this dummy target was counted in the same manner as the target in the beam. The initial activity of the dummy target was subtracted from the initial activity of the true target. Depending on the beam setup and the amount of shielding, this correction amounted to less than 5%, except for the data at 53, 60, and 1610 MeV. At these three energies, the absolute magnitude of the dummy activity was less than in the other cases, but the total initial activity was so low that the correction was as much as 20%.

Because the scintillator targets were thick, secondary particles (neutrons and protons) produced by nuclear interactions of the pions with upstream target nuclei could cause the production of C^{11}. The correction for this effect was found experimentally by measuring the cross section as a function of Lucite thickness placed before counter B and the target. The measured cross section increased with increasing Lucite thickness, so the correction for finite-source thickness was found by a linear extrapolation of the cross section to zero-target thickness. This correction was found to be 2 ± 1 mb at an incident pion energy of 215 ± 37 MeV.[8] The same secondary correction was used at other bombarding energies. Evaporation nucleons do not contribute to the formation of C^{11} because of the large binding energy

[8] The procedure used here for the secondary correction differs from that used in previous reports of this work. The final cross sections listed here are slightly different from the values given in Ref. 13 and in Paul L. Reeder and Samuel S. Markowitz, Bull. Am. Phys. Soc. 8, 69 (1963).

TABLE II. Cross sections for the reactions $C^{12}(\pi^-,\pi^-n)C^{11}$.

Energy of incident pion (MeV)	Cross sections (mb)					Average cross sections (mb)	Physics group Acknowledgment[d]
53±5	1.0					1±1	(1)
60±6	8.8	9.0				9±2	(1)
80±8	40.1	35.3				38±4	(2)
127±11	58.6	58.9	58.2			59±5[a]	(3)
179±10	69.7	67.2				68±6	(4)
212±10	66.6	67.8	67.7			67±6	(4)
245±10	59.4	62.6	62.5			61±6	(4)
304±9	40.8	43.9	39.6			41±4	(5)
342±10	38.4	33.7				36±4	(6)
373±10	28.6	29.6	29.4	28.4	29.5		
	32.3	30.9	30.6	30.1		30±3	(6)
423±10	17.9	21.7	21.8	36.6		25±8	(6)
1610±20	18.9					19±5[b]	(7)
1000	18					18[c]	

[a] The pion beam was monitored by means of a calibrated ion chamber.
[b] See Sec. II C for discussion of beam monitor at this energy.
[c] This datum is from A. M. Poskanzer, J. B. Cumming, G. Friedlander, J. Hudis, and S. Kaufman, Bull. Am. Phys. Soc. **6**, 38 (1961).
[d] See Acknowledgment section of text.

(18.3 MeV) of a neutron in C^{12}; hence, only fast secondary nucleons can produce C^{11}. These high-energy secondaries come from pion-absorption processes and fast-cascade collisions within nuclei.

III. RESULTS

A. Cross Sections

The cross sections were calculated from the expression

$$\sigma = D_0/nI(1-e^{-\lambda t}),$$

where D_0 is the disintegration rate at end-of-bombardment time, n is the number of target carbon nuclei per cm^2, I is the pion intensity in π per min, λ is the decay constant for C^{11} (corresponding to $t_{1/2}=20.4$ min), and t is the duration of bombardment in min. Bombardment times were usually of the order of one half-life. Fluctuations in beam intensity during this time were small, so the average pion intensity over the entire bombardment time was used for I. The quantity D_0 was obtained from the counting rate at end of bombardment after correcting for the positron-detector efficiency of 83%. The positron branching ratio was taken to be 100%. The plastic scintillator is nominally polystyrene (CH) and contains 91.54% carbon by weight. No attempt was made to distinguish between the production of C^{11} from C^{12}(98.9%) and from C^{13}(1.1%); the cross sections were calculated for the production of C^{11} from both isotopes.

The corrected cross sections are presented in Table II and the $C^{12}(\pi^-,\pi^-n)C^{11}$ excitation function is shown in Fig. 4 together with the π^-n free-particle cross sections.[8] The first column of Table II gives the incident-pion energy at the midpoint of the plastic-scintillator target. The pion energies of 179 and 212 MeV were obtained by placing Cu, 2 in. and 1 in. thick, respectively, in the 245-MeV beam. The energy of 342 MeV was obtained by placing 1 in. of Cu in the 373-MeV beam. The uncertainty listed with the pion energy is compounded of the energy spread of the beam and the energy spread in passing through the target. The second column of Table II presents the corrected cross sections for the individual bombardments. Column three gives the average value of the cross section and the estimated uncertainty. The number in the final column refers to the physics group (see Acknowledgments) whose pion beam was used. Also included in this table is a measurement at 1.0 BeV made at Brookhaven by use of a similar technique.

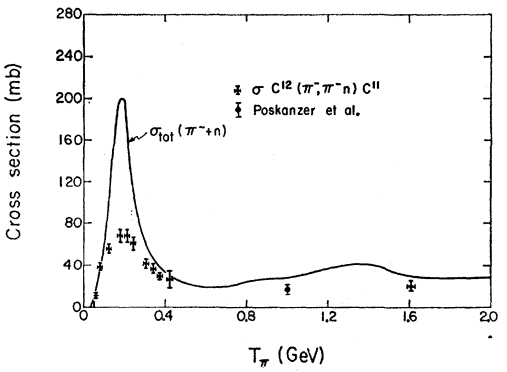

FIG. 4. Cross section for $C^{12}(\pi^-,\pi^-n)C^{11}$ reaction plotted versus incident-pion energy. The smooth curve is the total cross section for π^-n scattering, which is equal to the total cross section for π^+p scattering by charge symmetry. (Poskanzer *et al.*, see Table II, Ref. c).

B. Errors

The error associated with the cross section was calculated from the uncertainties in the following factors.

(1) The efficiency of the C^{11} detector was (83±3)% and was the same for all bombardments.

(2) The production of C^{11} by secondaries in the target was taken to be 2±1 mb at all bombarding energies.

(3) The contribution to C^{11} activity from stray background at the accelerator was about (20±5)% at 53, 60, and 1610 MeV, and less than (5±1)% at other energies.

(4) The correction for muon contamination in the pion beam was (35±5)% at 53 and 60 MeV, but decreased to about (8±1)% at 373 MeV.

(5) The uncertainty in the determination of the initial activity depended on the intensity of the pion beam. The 53-, 60-, and 1610-MeV beams had low intensities and consequently the C^{11} decay curves were extrapolated with an accuracy of about 15% for the initial activity. At other energies the initial activity could be determined with an uncertainty of less than 5%.

(6) The *maximum* correction for "accidentals" in the counting of the pion beam was (10±2)% but in most cases the correction and associated uncertainty was much less.

The average of the uncertainties for individual determinations was combined by root-mean-square

addition with the standard deviation of the average cross section in order to obtain the uncertainty listed with the average cross section in column three of Table II.

IV. DISCUSSION

The principal feature in the $C^{12}(\pi^-,\pi^-n)C^{11}$ excitation function is the peak at about 190 MeV. This corresponds to the same energy as the resonance peak in free-particle π^-n scattering. We now wish to discuss several possible mechanisms for the $C^{12}(\pi^-,\pi^-n)C^{11}$ reaction to determine the cause of the peak in the excitation function.

A. Compound Nucleus

The compound-nucleus mechanism requires the bombarding particle to be completely absorbed by the target nucleus. The kinetic energy of the projectile is then shared among all the nucleons, resulting in a highly excited nucleus. After a relatively long time the nucleus de-excites by emission of the necessary particles and γ rays.

Pion absorption is distinct from the usual concept of nucleon absorption in the compound-nucleus sense. Absorption of a pion takes place between two nucleons within the nucleus, and the rest-mass energy of the pion is converted into kinetic energy of the absorption partners. The pion rest-mass energy of 140 MeV provides a great deal of excitation energy and causes severe disruption of the nucleus. For the particular reactions studied here, absorption of a π^- can not lead to C^{11} because the "compound system" has $Z=5$. Hence C^{11} is not produced from C^{12} plus π^- by the compound-nucleus mechanism.

B. Two-Step Mechanism

Spallation reactions of protons at high energy have often been interpreted in terms of a cascade-evaporation model.[9] The nuclear reaction is presumed to occur in two stages. The first stage is a "cascade" of fast two-body collisions, with some nucleons being emitted immediately. The end of the cascade stage leaves a highly excited nucleus which then de-excites in a manner similar to the compound nucleus—by evaporation of nucleons and by γ-ray emission.

The $C^{12}(\pi^-,\pi^-n)C^{11}$ reaction can occur by a special application of this model which we define as the two-step mechanism. In this two-step mechanism the incident particle undergoes a fast collision with a single nucleon, and one of the collision partners escapes the nucleus without further interactions; the other collision partner shares its recoil energy with the other nucleons and the resultant nuclear excitation eventually leads to evaporation of one nucleon. The initial collision may be with either a proton or a neutron. For the $C^{12}(\pi^-,\pi^-n)C^{11}$ reaction to occur, the incident pion must be the collision partner that escapes the nucleus immediately.

[9] J. M. Miller and J. Hudis, Ann. Rev. Nucl. Sci. **9**, 159 (1959).

C. One-Step Mechanism

The one-step mechanism or pure knock-on mechanism is similar to the two-step mechanism except that both collision partners escape the nucleus immediately after the collision and without any other interactions. The nucleus cannot be excited to the point of evaporating additional nucleons. For a (π^-,π^-n) reaction the initial collision can be only with a neutron. Singh and Alexander have shown that the $C^{12}(p,pn)C^{11}$ reaction proceeds by this mechanism in the proton energy range from 0.25 to 6.2 GeV.[10]

D. Isobar Formation

The (π^-,π^-n) reaction might also proceed through the formation of a pion-nucleon isobar which then escapes the nucleus without exciting the nucleus to emit additional particles.[11] The isobar is a resonant state of a pion and nucleon and has a lifetime determined from the width of the resonance Γ and the uncertainty principle $\tau=\hbar/\Gamma$. This lifetime is comparable to the time the isobar takes to cross the nucleus, about 10^{-23} sec. The Monte Carlo calculations being made at Brookhaven assume that all pions form isobars after their first collision in nuclear matter.[12] The adequacy of this model has not yet been proved. The (π^-,π^-n) reaction could possibly be a test of the accuracy of the isobar model for nuclear reactions.

V. CALCULATIONS

The exact mathematical treatment of even the simple nuclear reactions is an extremely complicated affair. However, two approximate calculations, based on the one-step and two-step mechanisms, were performed in an attempt to determine the mechanism of the C^{12}-$(\pi^-,\pi^-n)C^{11}$ reaction. A calculation based on the isobar mechanism would be similar to the calculation based on the one-step mechanism, but was not attempted in this work because the cross sections and angular distributions for isobar scattering inside the nucleus are not known.

The nuclear model used for these calculations was that of a degenerate Fermi gas with a square-well density distribution. The nucleon density ρ was assumed to be constant out to the nuclear radius R at which point the density dropped sharply to zero. For the C^{12} nucleus, we used $R=3.04$ F and $\rho=1.02\times10^{38}$ nucleons/cm^3. The following sections discuss the calculations briefly—more complete details are given elsewhere by Reeder.[13]

[10] S. Singh and J. Alexander, Phys. Rev. **128**, 711 (1962).
[11] Z. Fraenkel, Phys. Rev. **130**, 2407 (1963).
[12] J. M. Miller and G. Friedlander (private communication).
[13] Paul L. Reeder, Ph.D. thesis, University of California, Lawrence Radiation Laboratory Report UCRL-10531, 1962 (unpublished).

A. Two-Step Calculation

As discussed previously, the two-step mechanism assumes that the pion interacts with just one nucleon and then escapes from the nucleus. The recoil energy of the struck nucleon is converted into nuclear excitation energy and the nucleus eventually deexcites by evaporating just one neutron. We will ignore the possibility of the pion undergoing two collisions and escaping after leaving just enough excitation energy to evaporate one neutron.

The cross section can be approximated by

$$\sigma(\pi^-,\pi^-n)=\int_{\text{vol}} P(\pi^-,\pi^-n)=P_1P_T\sigma_{\text{geom}}\,, \qquad (1)$$

where P_1 is the probability that the incident particle makes one and only one collision in passing through the nucleus, P_T is the probability that the struck particle receives a recoil energy sufficient to evaporate only one particle, and σ_{geom} is the geometrical cross section of the C^{12} nucleus.

An analytic expression for P_1 has been given by Markowitz with the approximation that the incident particle scatters at 0 deg and continues on with the same mean free path as before the collision[14]:

$$P_1=\frac{\lambda^2-\exp(-2R/\lambda)[2R^2+2R\lambda+\lambda^2]}{R^2}, \qquad (2)$$

where R is the nuclear radius and λ is the mean free path. This expression is not valid below the 190-MeV resonance region but becomes more accurate as the GeV region is reached. From the definition of P_T, the range of excitation energies due to the initial π^-n collision must be greater than the neutron binding energy of 18.3 MeV, but not great enough to evaporate a second particle. The pion scattering angles corresponding to the nucleon recoil energies of 19 and 29 MeV were calculated from the relativistic equations given by Morrison.[15] The angular distributions for π^-n elastic scattering were integrated between the two angles and divided by the total elastic-scattering cross section to obtain the fraction of events that left the correct amount of excitation energy. This approximation overestimates the (π^-,π^-n) contribution because for a given excitation energy there is competition from proton evaporation.

The geometrical cross section approximates the integration over the nuclear volume for the probability of a (π^-,π^-n) event. The geometrical cross section was calculated from πR^2 which, for the value of $R=3.04$ F, gives $\sigma_{\text{geom}}=290$ mb for C^{12}.

B. One-Step Calculation

The one-step mechanism can be described by the general expression

$$P(\pi^-,\pi^-n)=P_iP_{\text{coll}}P_\pi P_n\,, \qquad (3)$$

where $P(\pi^-,\pi^-n)$ is the probability for occurrence of a (π^-,π^-n) reaction at a given location in the nucleus, P_i is the probability of an incident pion's reaching that location, P_{coll} is the probability of a π^-n collision at that location, P_π is the probability that the recoil pion escapes unscathed, and P_n is the probability that the struck neutron is emitted.

P_i and P_π are functions only of the pion mean free path and the distance the pion travels in nuclear matter. We define

$$P_i=\exp(-x/\lambda_i) \qquad (4)$$

and

$$P_\pi=\exp(-s_\pi/\lambda_\pi)\,, \qquad (5)$$

where x is the distance the incoming pion must travel in nuclear matter before the collision, λ_i is the mean free path of the pion before the collision, s_π is the distance the outgoing pion must travel, and λ_π is the mean free path of the outgoing pion. Likewise, P_n is given by

$$P_n=\exp(-s_n/\lambda_n)\,, \qquad (6)$$

where s_n is the distance the outgoing neutron must travel in nuclear matter, and λ_n is the neutron mean free path. The expression for the probability of a collision, P_{coll}, is given by

$$P_{\text{coll}}=1-\exp(-\Delta x/\lambda_{\pi^-n})\,, \qquad (7)$$

where Δx is a small increment of distance along the pion path length and λ_{π^-n} is the mean free path between π^-n collisions. The nucleon mean free paths were calculated using effective nucleon-nucleon cross sections obtained from Winsberg and Clements.[16] Mean free paths for pions were estimated in a manner similar to that of Frank, Gammel, and Watson.[17]

The outgoing distances s_π and s_n are strongly dependent on the location of the collision and on the scattering angle θ. The average distance traveled by the outgoing pion was approximated by averaging the two distances corresponding to the given scattering angles θ and $-\theta$ in the plane defined by the beam path and the center of the nucleus. The same procedure was used to find the average distance the neutron travels through nuclear matter for a given pion scattering angle.

The probability for a (π^-,π^-n) event at the point (i,j), where i is the impact parameter and j is the distance traveled before the collision, is found by sub-

[14] Samuel S. Markowitz, Ph.D. thesis, Princeton University, 1957 (unpublished).

[15] P. Morrison, *Experimental Nuclear Physics*, edited by E. Segre (John Wiley & Sons, Inc., New York, 1953), Vol. II, Part VI, pp. 3–11.

[16] Lester Winsberg and Thomas P. Clements, Phys. Rev. **122**, 1623 (1961).

[17] R. M. Frank, J. L. Gammel, and K. M. Watson, Phys. Rev. **101**, 891 (1956).

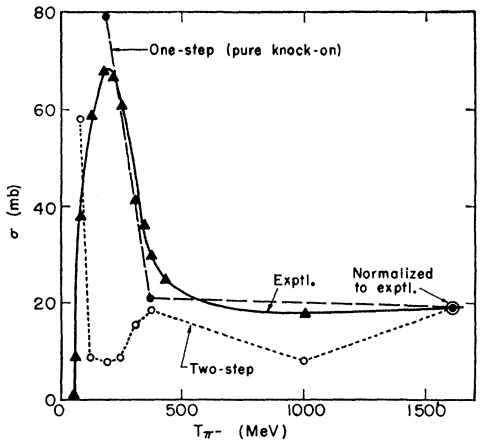

FIG. 5. Comparison of experimental and calculated $C^{12}(\pi^-,\pi^-n)C^{11}$ excitation functions. Solid curve is experimental. Dashed curve connects the cross sections calculated on the one-step model. The dotted curve connects the points calculated on the two-step model. Both calculated curves have been normalized to the experimental curve at 1610 MeV.

stituting in Eq. (3):

$$P(i,j)=P(\pi^-,\pi^-n)=P_iP_{\text{coll}}P_\pi P_n,$$
$$P(i,j)=\exp(-x/\lambda_i)[1-\exp(-\Delta x/\lambda_{\pi^-n})]\times\exp(-s_\pi/\lambda_\pi)\exp(-s_n/\lambda_n). \quad (8)$$

To obtain the cross section, $P(i,j)$ must be integrated along the path length x, weighted by $2\pi ada$ to account for the cylindrical symmetry, and integrated over da (da represents intervals along the impact-parameter coordinate).

The recoil energies and mean free paths are dependent on how one accounts for the angular dependence of π^-n scattering. For a complete calculation at a particular incident-pion energy, the (π^-,π^-n) cross section should be calculated for each scattering angle θ, weighted by the probability of having a scattering event at that angle, and then integrated over all the scattering angles. As a rough approximation to this procedure, the (π^-,π^-n) cross section was calculated for only three scattering angles, $\theta_{\text{c.m.}}=0$, 90, and 180 deg.

The above calculation was performed at three energies, 190, 370, and 1600 MeV, chosen to illustrate the main features of the experimental excitation function.

VI. CONCLUSIONS

A. Calculated Excitation Functions

The nuclear model and calculations performed here are simple and preliminary treatments of the C^{12}-$(\pi^-,\pi^-n)C^{11}$ reaction. Figure 5 shows the comparison of the calculated excitation functions for the one-step and two-step mechanisms together with the experimental excitation function. The results of the one-step calculation were multiplied by 5.6 and the results of the two-step calculation were multiplied by 1.7 in order to normalize the calculated excitation functions to the experimental excitation function.

The energy dependence of the two-step mechanism is distinctly different from the experimental excitation function. This means the two-step mechanism is not the cause of the peak in the $C^{12}(\pi^-,\pi^-n)C^{11}$ excitation function. It is possible that the two-step mechanism is increasing in importance at energies below the resonance peak, but our calculation is not expected to be valid in this region.

The one-step calculations did reproduce the correct shape for the excitation function. The one-step calculation was not attempted at energies below the resonance peak because the mean free path of the recoiling neutron was not sufficiently well known for very low recoil energies.[1] However, the strong dependence of the one-step calculation on the free-particle cross section, particularly in the term P_{coll}, makes it highly probable that the calculated $C^{12}(\pi^-,\pi^-n)C^{11}$ cross sections would decrease, in conformity with the free-particle cross sections.

The calculated cross sections from the one-step mechanism were lower than the experimental cross sections by a factor of about 5 or 6. The use of a square

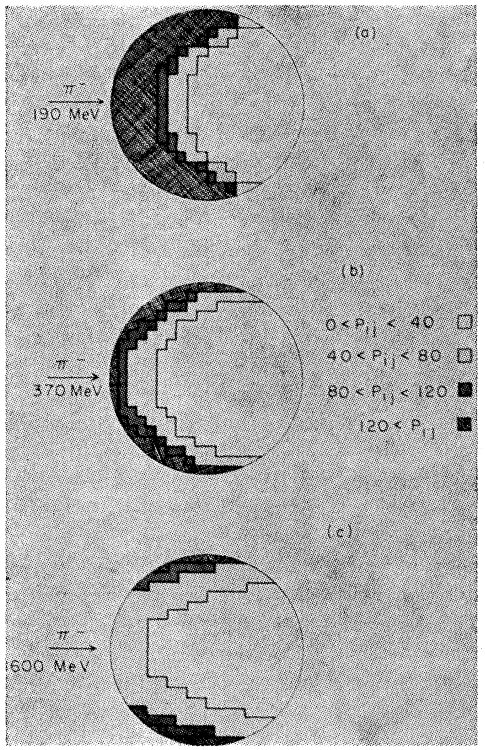

FIG. 6. Location of (π^-,π^-n) events after integration over the scattering angle θ. P_{ij} represents the relative probability of a (π^-,π^-n) event (calculated from $P_{ij}=P_iP_{\text{coll}}P_\pi P_n$) after weighting by angular distribution. (a) Incident pion energy is 190 MeV; (b) incident pion energy is 370 MeV; (c) incident pion energy is 1600 MeV.

well for the nucleon density may be a major cause of this discrepancy. Monte Carlo calculations that include a square well do not predict the correct magnitudes of the (p,pn) reactions.[18,19] Although our calculation is not a Monte Carlo calculation, the one-step calculation should also be done with a more accurate nucleon-density function because the simple reactions are very sensitive to the shape of the nuclear surface.

Another explanation for the low values of the calculated cross sections may lie in the isobar model. If the mean free paths of isobars in nuclear matter are not very different from nucleon mean free paths, the isobar mechanism predicts larger cross sections for the (π^-,π^-n) reaction than the one-step mechanism. Refinements of this calculation might provide information on the isobar cross sections in nuclear matter.

B. Location of (π^-,π^-n) Events

The one-step calculation also gave information on the relative probability of a (π^-,π^-n) event at different locations in the nucleus, as shown in Fig. 6 for the three different energies. The figure shows the value of P_{ij} for each location after weighting by the angular distribution. From the figure we note that the (π^-,π^-n) reaction occurs predominantly on the upstream surface and pole tips of the C^{12} nucleus. A quantitative estimate of the depth of this surface region is uncertain because of the approximations in the model and calculation. However, we estimate that about half the (π^-,π^-n) events occurred in a surface region whose depth was less than 0.2 of the nuclear radius.

The calculation done here for the (π^-,π^-n) reaction indicates that this reaction occurs on the upstream surface, in contrast to the calculation by Benioff for (p,pn) reactions at GeV energies.[20] Benioff's results showed that the (p,pn) reaction was predominantly from the downstream surface of the nucleus.

For our calculation, the distance the pion travels in nuclear matter is the feature controlling the location of the (π^-,π^-n) reaction, because the mean free path of the pion is generally either considerably smaller than or about equal to the mean free path of the neutron. The pion travels the shortest distance when the collision occurs on the upstream surface, because of the dominance of 180-deg scattering in our calculation. For a scattering angle of 180 deg, the neutron receives its greatest recoil energy and has the greatest probability of escaping without interacting with other nucleons. In addition, the angular distributions give more weight to 180-deg events than to 90-deg events.

The assumption in our calculation that the two-body reaction plane passes through the center of the nucleus overestimates the distance the recoil particles travel in nuclear matter. This effect is greatest for large impact parameters, and distorts the contour maps as well as decreases the calculated cross sections. Elimination of this defect might lead to even greater contributions from the pole-tip regions.

C. Resonance Broadening

The full width at half-maximum (FWHM) of the $C^{12}(\pi^-,\pi^-n)C^{11}$ peak is about 270 MeV; in comparison, the FWHM of the π^-n peak is about 145 MeV. The greater width of the (π^-,π^-n) peak is probably due to the fact that the struck neutron is moving rapidly within the potential well of the C^{12} nucleus. On the basis of the one-step mechanism, only the $p_{3/2}$ neutrons of C^{12} contribute to the (π^-,π^-n) reaction because removal of a $s_{1/2}$ neutron leaves the nucleus with too much excitation energy to prevent particle evaporation. If we assume that the $p_{3/2}$ momentum distribution is the same for neutrons and protons, we can use the data of Garron *et al.* to estimate the resonance broadening due to the neutron momentum distribution.[21] This calculation is based on the energy shift needed to maintain the same total energy of the system in the center-of-mass frame of reference for the case of a stationary nucleon and the case of a moving nucleon. For an average $p_{3/2}$-state momentum of 150 MeV/c, we estimate that the π^-n resonance should be broadened by about 100 MeV to give a FWHM of 245 MeV for the (π^-,π^-n) peak.[13] The agreement with the experimental width is satisfactory if one considers the errors in both the calculated and experimental widths.

In summary, the peak at 190 MeV in the $C^{12}(\pi^-,\pi^-n)$-C^{11} excitation function corresponds to the resonance peak in the free-particle π^-n scattering. This peak gives additional evidence for the occurrence of quasifree-particle scattering within the nucleus. Furthermore, we conclude that the pion-nucleon forces which act in free-particle scattering are not strongly modified when the nucleon is bound in nuclear matter.

ACKNOWLEDGMENTS

We are extremely grateful to the following individuals for providing meson beams: (1) W. C. Bowman, J. B. Caroll, J. A. Poirer, and M. Pripstein; (2) R. Beck, N. Dairiki, and T. Maung; (3) B. Czirr; (4) H. Goldberg, and R. W. Kenney; (5) N. Booth, R. Hill, H. Rugge, and O. Vik; (6) B. C. Barish, R. J. Kurz, J. Solomon, and V. Perez-Mendez; and (7) T. Eliof, W. Johnson, C. E. Wiegand, and T. Ypsilantis.

In addition, we would like to thank Owen Chamberlain for the bombardment with the external proton beam and Richard N. Chanda for the use of the "fast-slow" coincidence apparatus. We are indebted to the Moyer physics group for the loan of a discriminator and scale-of-eight unit. Fruitful discussions with Gerhart Friedlander are also gratefully acknowledged.

[18] N. Metropolis, R. Bivins, M. Storm, J. M. Miller, G. Friedlander, and A. Turkevich, Phys. Rev. **110**, 204 (1958).
[19] S. Markowitz, F. Rowland, and G. Friedlander, Phys. Rev. **112**, 1295 (1958).
[20] P. Benioff, Phys. Rev. **119**, 324 (1960).
[21] J. Garron, J. Jacmart, M. Riou, C. Ruhla, J. Teillac, and K. Strauch, Nucl. Phys. **37**, 126 (1962).

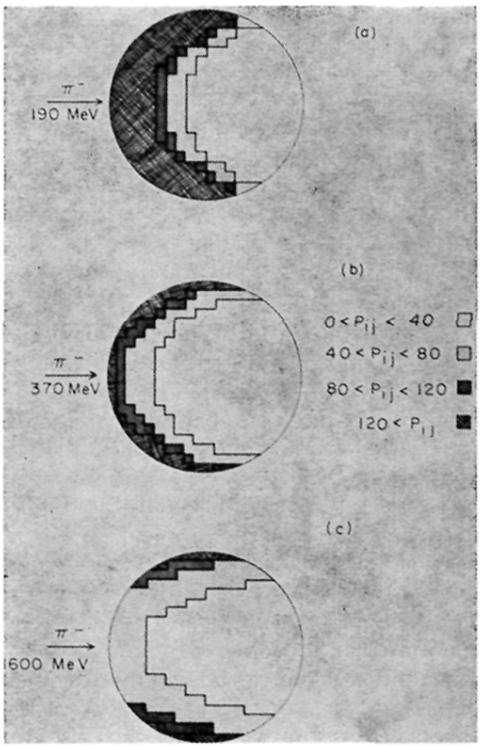

FIG. 6. Location of (π^-,π^-n) events after integration over the scattering angle θ. P_{ij} represents the relative probability of a (π^-,π^-n) event (calculated from $P_{ij}=P_iP_{\text{coll}}P_\pi P_n$) after weighting by angular distribution. (a) Incident pion energy is 190 MeV; (b) incident pion energy is 370 MeV; (c) incident pion energy is 1600 MeV.